10330 *J. Phys. Chem. A* **2006,** *110,* 10330−10335

Theoretical Study of Two-Photon Absorption in Donor−Acceptor Chromophores Tetraalkylammonium Halide/Carbon Tetrabromide

Juan Shen, Wen-Dan Cheng,* Dong-Sheng Wu, You-Zhao Lan, Fei-Fei Li, Shu-Ping Huang, Hao Zhang, and Ya-Jing Gong

State Key Laboratory of Structual Chemistry, Fujian Institute of Research on the Structure of Matter, the Chinese Academy of Sciences, Fuzhou, Fujian 350002, People's Republic of China

Received: May 21, 2006; In Final Form: June 28, 2006

Two-photon absorption properties of a series of donor−acceptor chromophores of tetraalkylammonium halide/carbon tetrabromide ([$NR_4h\cdot CBr_4$], h = Cl, Br, I; R = Me, Et, Pr) complexes are investigated in terms of the calculated results by the time-dependent density functional theory (TDDFT) technique combined with the sum-over-states (SOS) method. The modeling two-photon absorption spectra show that these charge-transfer complexes have large two-photon absorption (TPA) cross sections and the [$NEt_4I\cdot CBr_4$] has the largest TPA cross section δ with the value of 5.0×10^{-45} cm^4 s photon^{-1}. The maximum values of δ increase with increasing separations between the donor/acceptor in the order Cl···Br < Br···Br < I···Br for [$NEt_4h\cdot CBr_4$] complexes; however, the TPA cross sections δ vary slightly as the size of the alkyl group increases from methyl to propyl for the bromide as a donor, and the maximum wavelength of the TPA peak λ_{max} indicates a bathochromic shift. The charge transfers from the halide anion to the carbon tetrabromide make a significant contribution to the excited states, and the donor−acceptor charge transfer plays an important role in the TPA activity, whereas changes in size of alkyl group do not make a substantial contribution to TPA.

1. Introduction

Over the past few years, the two-photon absorption (TPA) process has gained the subject[1−6] of fast-growing interest in fields such as chemistry, photonics, and biological imaging, due to a number of potential applications including optical power limitation,[7,8] two-photon laser scanning microscopy,[9−11] deep tissue-penetrating photodynamic therapy,[12] three-dimensional micro- and nanofabrication,[13−15] and high-density optical data storage.[16,17] These applications are primarily based on accessing higher energy excited states using relatively low-energy laser sources. The potential applications have inspired a broad quest searching for functional chromophores with large TPA cross sections[18−21] and has stimulated research on the design, synthesis, and characterization of new molecules with large two-photon absorptivities.[22,23]

TPA is defined as the electronic excitation of a molecule or material induced by a simultaneous absorption of two photons of the same or different energies, which is one of the first nonlinear processes to be observed experimentally, shortly after the advent of lasers.[24] When a material instantaneously absorbs two lower energy photons than needed for one-photon (a linear) absorption, the two photons of longer wavelength are simultaneously absorbed by a chromophore, and the latter would normally be excited by a single photon with a shorter wavelength. TPA materials provide an advantage by excitation in the lower energy near-IR region resulting in the inherent higher energy photophysical properties of the chromophore. TPA prevents the damage of material as a result of a higher energy photon.[25]

A variety of two-photon chromophores including quasi-linear quadrupolar molecules symmetrically substituted with donor (D) and/or acceptor (A) groups (of the type D−π−D, A−π−A, D−A−D, and A−D−A) incorporating a variety of conjugated bridges,[18,22,23,26,27] bifluorene and polyfluorene systems,[28] various dipolar conjugated D−A molecules,[18] multibranched compounds,[29,30] dendrimers,[31] and organometallic complexes[32] have been synthesized and their structure−property relationships established. These studies reveal that the molecular structure has a significant influence on the TPA cross section of the molecules and the charge transfer effectively enhances the two-photon absorptivity.[23] Consequently, there is a great requirement to further understand the structure−property relationships regarding excited-state dynamics (transition moments, electronic coupling between levels, molecule interactions). The development can benefit the design of materials increasing the TPA cross section of molecules and tuning the position of the TPA peak. Carbon tetrabromide (CBr_4) as a prototypical electron acceptor forms intermolecular complexes with one-dimensional donors,[33,34] for which the charge-transfer nature has been revealed in a series of physical−chemical studies.[35,36] Kochi and co-workers[34] studied the electronic coupling and charge-transfer nature of a series of electronically coupled donor/acceptor diamondoid networks formed by carbon tetrabromide and electron-rich halide anions (chloride, bromide, and iodide). They indicated that these diamondoid charge-transfer associates possess unusual nonlinear optical properties. To understand the influence of charge transfers upon TPA, we will aim to theoretically investigate the excitation-state properties of halide salts and carbon tetrabromide electron-donor/acceptor dyads and discuss the TPA properties of these complexes.

2. Computational Procedures

The frequency-dependent third-order polarizabilities and two-photon absorption cross section $\delta(\omega)$ were calculated by employing the time-dependent density functional theory (TDDFT),[37−39] using the Gaussian 03 package and the B3LYP functional combined with the sum-over-states (SOS) method.[40,41] Standard basis sets 6-31+G** were chosen to describe C, H, and N atoms.

10.1021/jp063108v CCC: $33.50

The 3-21G** basis set was used for the halogen atoms. The treatment of electron−electron interactions (EEI) is included in a natural way in the TDDFT calculations.[42] The validity that the TDDFT/B3LYP method is employed to compute excitation energy and frequency-dependent response functions of γ was described in refs 43 and 44.

The two-photon absorption coefficient (β) can be shown to be proportional to the imaginary part of the third-order susceptibility tensor. Thus, the molecular two-photon absorption cross section $\delta(\omega)$ can be characterized by the imaginary part of the molecular third-order nonlinear polarizability, defined at the absorption frequency of ω, Im $\gamma(-\omega;\omega,\omega,-\omega)$,[45] through the following equation:

$$\delta(\omega) = 8\pi^2\hbar\omega^2/(n^2c^2)L^4\ \mathrm{Im}\ \gamma(-\omega;\omega,\omega,-\omega) \qquad (1a)$$

where $\hbar$ is Planck's constant divided by 2π, n denotes the refractive index of the medium (vacuum assumed for the calculations), L corresponds to the local-field factor (equal to 1 for vacuum), and c is the speed of light. By the relation of $\omega = 2\pi c/\lambda$, eq 1a is simply described by

$$\delta(\omega) = 32\pi^4\hbar/(n^2\lambda^2)L^4\ \mathrm{Im}\ \gamma(-\omega;\omega,\omega,-\omega) \qquad (1b)$$

Here, λ is wavelength. The unit of $\delta(\omega)$ will be cm^4 s photon^{-1}, if cgs units are used for $\hbar$ and λ, and esu is the unit for $\gamma(-\omega;\omega,\omega,-\omega)$. Noted here γ (esu) = γ (cm^6 erg^{-1}). We calculate Im $\gamma(-\omega;\omega,\omega,-\omega)$ using the sum-over-states (refs 40 and 41) expression. The SOS formula can be divided into two terms of summations, as shown in ref 46; the first summation involves the two-photon allowed states, and the second summation involves one-photon allowed states. Because the calculations of $\delta(\omega)$ only involve the two-photon states, the third-order polarizability of two-photon resonance enhancement in degenerate four-wave mixings leaves behind only the first term and can be written as

$$\gamma_{abcd}(-\omega;\omega,\omega,-\omega) = 3/4(2\pi/h)^3e^4{\sum}'_j(\omega_{jo} - 2\omega - i\Gamma_{jo})^{-1}$$
$$\Big[{\sum}'_k(\langle o|r_a|k\rangle\langle k|r*_b|j\rangle + \langle o|r_b|k\rangle\langle k|r*_a|j\rangle)/(\omega_{ko} - \omega)$$
$${\sum}'_i(\langle j|r*_c|i\rangle\langle i|r_d|o\rangle + \langle j|r*_d|i\rangle\langle i|r_c|o\rangle)/(\omega_{io} - \omega)\Big] \qquad (2)$$

Then, we take out the imaginary part of this formula, and the orientational average, which is

$$\langle \mathrm{Im}\ \gamma\rangle = 1/5(\mathrm{Im}\ \gamma_{xxxx} + \mathrm{Im}\ \gamma_{yyyy} + \mathrm{Im}\ \gamma_{zzzz} + \mathrm{Im}\ \gamma_{xxyy} +$$
$$\mathrm{Im}\ \gamma_{xxzz} + \mathrm{Im}\ \gamma_{yyxx} + \mathrm{Im}\ \gamma_{yyzz} + \mathrm{Im}\ \gamma_{zzxx} + \mathrm{Im}\ \gamma_{zzyy}) \qquad (3)$$

In eq 2, the state $|j\rangle$ is a two-photon resonance state and the transition energy of this state satisfied the condition $\omega_{jo} - 2\omega = 0$. Γ_{jo} is a damping factor (line half-width broadening) directly related to the total dephasing rate of the various excited states, and which is assumed a constant parameter of $\hbar\Gamma = 0.01$ eV in our work. Here, in the calculations of third-order nonlinear optical properties, we are only concerned about contributions from electric dipole transitions because they are the most intense as compared with vibrational and rotational transitions.[47] In the following discussions, we will only give systematic comparisons of third-order nonlinear optical properties among the studied species and omit vibration and rotation contributions to polarizabilities or hyperpolarizabilities. The self-consistent field convergence criterions are set by the default values of the GAUSSIAN 03 program in the excited-state calculations. The core orbitals are frozen in the correlation calculations. The iterations of excited states are continued until the changes on energies of states are no more than 10^{-7} au between the iterations, and the convergence has been reached in all the calculations of excited states. In the calculation of γ, we use only about 50 excited states in the summations of SOS expansion and the convergence of γ has been reached well.

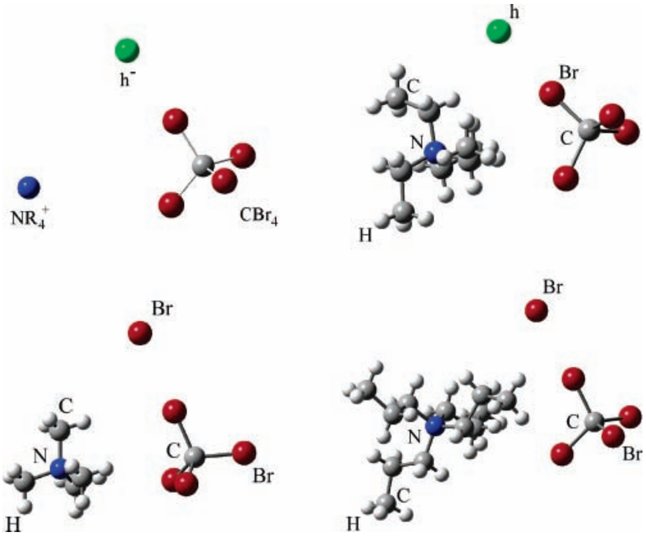

Figure 1. Chemical structure of electron donating-election accepting [NR$_4$h·CBr$_4$], (h = Cl, Br, I; R = Me, Et, Pr).

3. Results and Discussion

Donor−acceptor molecules constitute an important class of NLO chromophores. Key properties include large nonresonant hyperpolarizabilities arising from intermolecular donor to acceptor charge-transfer excitation. Figure 1 shows the structures of the molecules considered in this work. These complexes with carbon tetrabromide serve as electron acceptors and tetraalkylammonium halides serve as electron donors with the halide being chloride, bromide, and iodide, and the organic building element of progressively different sizes (alkyl = Me, Et, and Pr) form two series of donor/acceptor dyads with the structure character of an intermolecular [Br$_3$CBr···halide] association interaction.

Our calculation results of frequency-dependent TPA cross sections $\delta(\omega)$ of investigated compounds are plotted in Figure 2. The TPA cross sections $\delta(\omega)$ are calculated at wavelengths ranging from 400 to 1000 nm, and there is only one strong absorption peak that appears around 600 nm for all the considered species. Consequently, Figure 2 only gives wavelengths ranging from 450 to 750 nm in the absorption region, which represents a highlight of photophysical behavior. We list the values of the imaginary part of the second hyperpolarizability Im γ at the maximum absorption peak position $\lambda_{\max}$ for five complexes in Table 1. As shown, the charge-transfer complexes [NR$_4$h·CBr$_4$] (h = Cl, Br, I; R = Me, Et, Pr) of halide as the electron donor and carbon tetrabromide as the acceptor have large TPA cross sections and [NEt$_4$I·CBr$_4$] has the largest δ among them, the value of which reaches about 5.0 × 10^{-45} cm^4 s photon^{-1}. In the following, we will consider two series of charge-transfer complexes to monitor the structure−property relationship arising from (a) the nature of the halide donor and (b) the size of the tetraalkylammonium and discuss the behavior of two-photon resonant absorption.

For [NEt$_4$h,CBr$_4$] (h = Cl, Br, and I), the maximum values of the two-photon resonant absorption cross section δ increase with the increasing radii of the halide anions in the order of

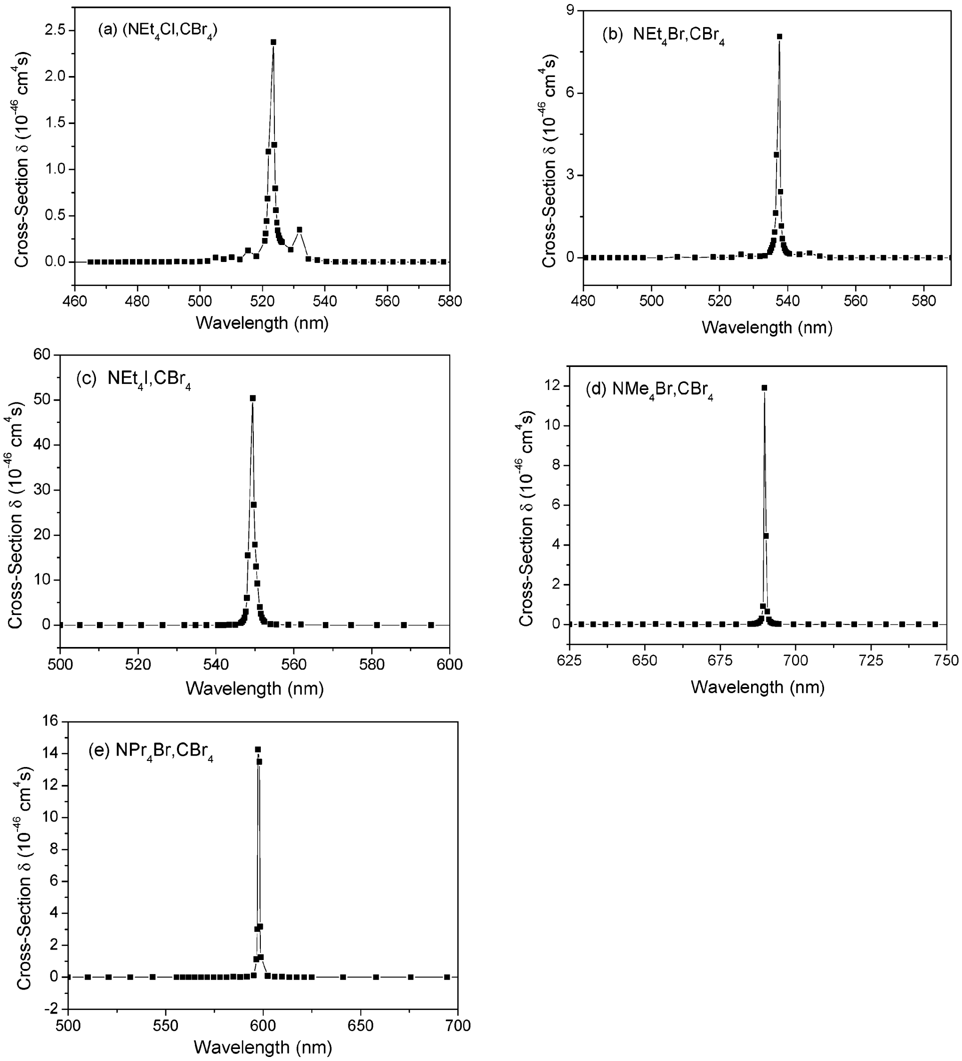

Figure 2. Calculated two-photon absorption cross section of [NR_4h,CBr_4] (h = Cl, Br, and I; R = Me, Et, and Pr) based on TDDFT at the B3LYP/6-31+G** level combined with SOS method.

TABLE 1: Calculated Wavelengths of Maximum Two-Photon Absorption Positions λ, Cross Sections δ (10^{-46} cm^4 s photon^{-1}) and Imaginary Part of the Second Hyperpolarizabilities Im $\gamma(-\omega;\omega,\omega,-\omega)$ (10^{-31} esu) of [$NR_4h\cdot CBr_4$] (h = Cl, Br, and I; R = Me, Et, and Pr) at TDB3LYP/6-31+G Model**

compound	λ_{max} (nm)	Im γ	δ	R_{DA} (Å)[a]
$NEt_4Cl\cdot CBr_4$	523.6	1.981	2.376	3.09
$NEt_4Br\cdot CBr_4$	537.6	7.086	8.059	3.15
$NEt_4I\cdot CBr_4$	549.5	46.29	50.408	3.30
$NMe_4Br\cdot CBr_4$	689.7	17.210	11.895	3.33
$NPr_4Br\cdot CBr_4$	597.4	15.475	14.255	3.19

[a] R_{DA} is the separation between the donor/acceptor as the distance of halide···Br.

$Cl^- < Br^- < I^-$. In fact, this finding also indicates that the two-photon absorptions δ increase with the increasing separate R_{DA} between the donor and acceptor. Table 1 lists the distances R_{DA} between the donor (h) and acceptor (Br in CBr_4). It is found that when the halogen donor varies from Cl to Br to I, the distance of the h···Br is 3.09, 3.15 and 3.30 Å, and the corresponding maximum TPA cross section δ is 2.376×10^{-46}, 8.059×10^{-46}, and 50.408×10^{-46} cm^4 s photon^{-1} for the $NEt_4h\cdot CBr_4$ complexes, respectively. Meanwhile, the δ values do not vary substantially for different sizes of alkyl groups ($NMe_4Br\cdot CBr_4$ and $NPr_4Br\cdot CBr_4$) despite different values of R_{DA} resulting from alkyl group space arrangements. The δ of [$NEt_4I\cdot CBr_4$] is 1 order of magnitude larger than the two others, and it is about 20 times δ for the h = Cl complex, as shown in Table 1. The largest δ value is localized at 520−550 nm, and the maximum TPA peak λ_{max} shows a bathochromic shift with increasing atomic order number of the halogen. For [NR_4Br,CBr_4] (R = Me, Et, and Pr), when the size of the alkyl group increases, the δ values are 11×10^4, 8×10^4, and 14×10^4 GM (1 GM = 10^{-50} cm^4 s photon^{-1}) at wavelengths of 690, 538, and 597 nm, respectively. The TPA cross sections vary slightly as compared with those for [NEt_4h,CBr_4] (h = Cl, Br, and I). Overall, for the investigated complexes [$NR_4h\cdot CBr_4$] (h = Cl, Br, I; R = Me, Et, Pr), the halide as the electron donor plays an important role for TPA activity (it has a strong influence on the TPA cross sections and the largest TPA cross sections increase with the donor strength), whereas changes in the size of the alkyl group make a small contribution. In Lindeman's work, they pointed out that the charge-transfer nature of (CBr_4, halide) complexes represents a factor potentially favorable for high second-order hyperpolarizability and the tetraalkylammonium counterions lead to optimal support of the diamondoid network of CBr_4 and halide by stabilizing the cavity void.[34] Our results are clearly consistent with their reports.

Furthermore, we will search the originations of large TPA cross sections $\delta(\omega)$ in the considered complexes. From eq 1a, we can see that the $\delta(\omega)$ value only depends on the imaginary part

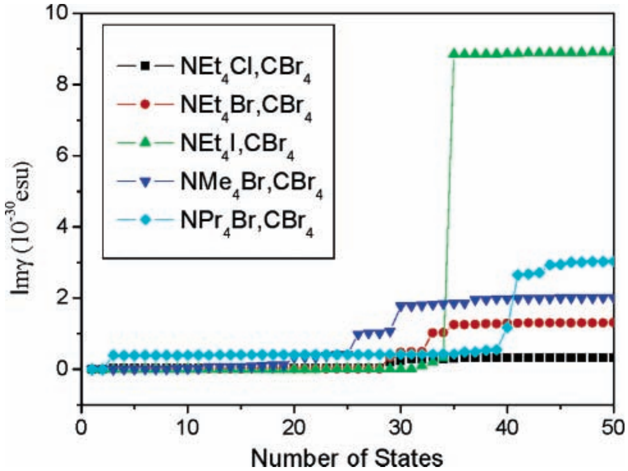

Figure 3. State-dependent Im $\gamma(-\omega;\omega,\omega,-\omega)$ at the character wavelength for complexes [NR$_4$h·CBr$_4$] (h = Cl, Br, I; R = Me, Et, Pr).

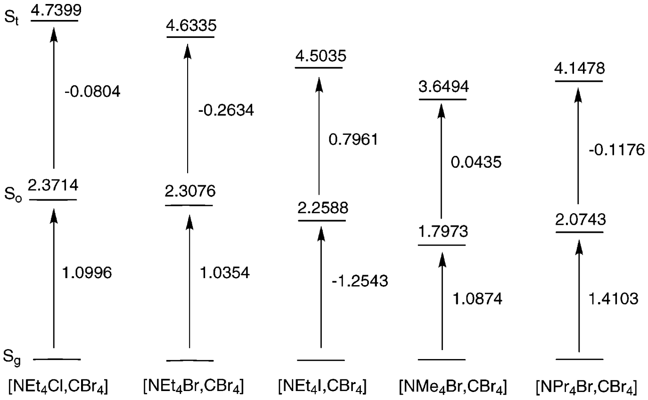

Figure 4. Scheme of the calculated energy levels and transition dipole moments (in eV and au units, respectively) at three state models for [NR$_4$h·CBr$_4$] (h = Cl, Br, I; R = Me, Et, Pr).

of the second hyperpolarizability, Im $\gamma(-\omega;\omega,\omega,-\omega)$, whereas the input frequency is given at the vacuum medium. Accordingly, the two-photon states contributing to Im $\gamma(-\omega;\omega,\omega,-\omega)$ shown in eq 2, also contribute to $\delta(\omega)$ value. Figure 3 presents the plots of Im $\gamma(-\omega;\omega,\omega,-\omega)$ values vs two-photon states at the characteristic wavelength (resonant wavelength). It is shown that the TPA cross sections are mostly contributed from one two-photon state.

For instance, state 31 of [NEt$_4$Cl,CBr$_4$], state 33 of [NEt$_4$Br,CBr$_4$], state 35 of [NEt$_4$I,CBr$_4$], state 27 of [NMe$_4$Br,CBr$_4$], and state 41 of [NPr$_4$Br,CBr$_4$], which are the TPA resonant states, have contributions of 86%, 78%, 99%, 51%, and 87% to the $\delta(\omega)$ values at wavelength of 524, 538, 550, 690, and 597 nm, respectively. The TPA state can be constructed by one-electron promotion from the ground state to the excited state *i* (one-photon state) by absorbing one-photon energy, and the electron promotion from state *i* to state *j* (two-photon state) by absorbing again one-photon energy. Table 2 lists the states involved in TPA processes. It means that two-photon resonant transition can be described by three-state model, as shown in Figure 4.

The peak two-photon resonant value of $\delta(\omega)$ is represented by

$$\delta_{g\to t} \propto (M_{go}{}^{2}M_{ot}{}^{2})/(E_o - E_g - \hbar\omega)^2\Gamma \qquad (4)$$

where the subscripts g, o, and t refer to the ground state and one- and two-photon states, respectively, and $\hbar\omega = (E_t - E_g)/2$. From formula 4, we can deduce two factors: (1) $\delta(\omega)$ value increases with the moment products ($M_{go}{}^2M_{ot}{}^2$), (2) $\delta(\omega)$ value increases as the one-photon detuning term ($E_o - E_g - \hbar\omega$) decreases. Table 2 summarizes the transition moments from ground state to one-photon states and from one-photon states to two-photon states, together with transition energies and incident photon energies. Approximately, the moment products of ($M_{go}{}^2M_{ot}{}^2$) increase and the one-photon detuning term ($E_o - E_g - \hbar\omega$) decreases as the size of the halide increases. Here, we note that the dipole moment of the transition is equivalent to an electron moving through distance. If the charge transfers between donor and acceptor have the same properties for [NEt$_4$h·CBr$_4$], the moment products of ($M_{go}{}^2M_{ot}{}^2$) depend only on the distance between the donor and acceptor. It is found from Tables 1 and 2 that the moment products are in proportion to the donor−acceptor distance of R_{DA} and the δ values increase as the moment products increase for the [NEt$_4$h·CBr$_4$] complexes. Accordingly, the three-state model well explain the distance-dependent two-photon absorption properties. However, the [NMe$_4$Br·CBr$_4$] is exceptable, for which the ($M_{go}{}^2M_{ot}{}^2$) is smaller compared with the values for other complexes, but its value of $\delta(\omega)$ has a substantially large one. This reason can be ascribed to the small detuning energy ($E_o - E_g - \hbar\omega$).

Table 3 lists the configuration components of TPA resonant states. For example, the TPA resonant state of [NEt$_4$Cl·CBr$_4$] has the greatest contribution from the configuration MO$_{118}$ → MO$_{129}$, where the molecular orbital MO$_{118}$ is occupied and orbital MO$_{129}$ is unoccupied. All the related orbitals of [NEt$_4$h·CBr$_4$] (h = Cl, Br, I) listed in Table 3 are plotted in Figure 5. It is found that the electronic transition between the halide anion and the carbon tetrabromide, namely, the charge transfer from the electron donor and acceptor, makes a significant contribution to the excited states. The occupied orbitals are mostly constructed by the p-type atomic orbitals of the halide ions, and the unoccupied ones are mainly formed by the p-type atomic orbitals of carbon tetrabromide group mixing with small s-type and p-type atomic orbitals of the C atoms on the alkyl group. However, note that with the push strength enhancement of the donor from Cl$^-$ to I$^-$ ions, the orbitals contributing to the

TABLE 2: Transition Moments and Energies between the One-Photon States

compound	→ state	moment (au)	($M_{go}{}^2M_{ot}{}^2$)	energy (eV)	ħω (eV)	detuning energy (eV)
NEt$_4$Cl·CBr$_4$	G → 3	1.0996	0.0078	2.3714	2.368	0.003
	3 → 31	−0.0804				
	G → 31			4.7399		
NEt$_4$Br·CBr$_4$	G → 3	1.0354	0.0744	2.3076	2.306	0.0016
	3 → 33	−0.2634				
	G → 33			4.6335		
NEt$_4$I·CBr$_4$	G → 3	−1.2543	0.9971	2.2588	2.256	0.0018
	3 → 35	0.7961				
	G → 35			4.5035		
NMe$_4$Br·CBr$_4$	G → 3	1.0874	0.0022	1.7973	1.798	0.0007
	3 → 27	0.0435				
	G → 27			3.6494		
NPr$_4$Br·CBr$_4$	G → 3	1.4103	0.0275	2.0743	2.076	0.0017
	3 → 41	−0.1176				
	G → 41			4.1478		

TABLE 3: Configuration Components of Two-Photon Resonant States

compound	state	largest configuration
NEt$_4$Cl·CBr$_4$	31	0.6318 (118→129)
NEt$_4$Br·CBr$_4$	33	0.5345 (128→140)
NEt$_4$I·CBr$_4$	35	0.4950 (135→147)
NMe$_4$Br·CBr$_4$	27	0.5768 (112→122)
NPr$_4$Br·CBr$_4$	41	0.6118 (142→156)

(a) orbitals of $[NEt_4Cl\cdot CBr_4]$

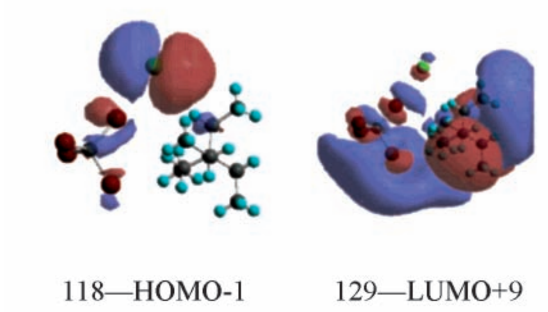

(b) orbitals of $[NEt_4Br\cdot CBr_4]$

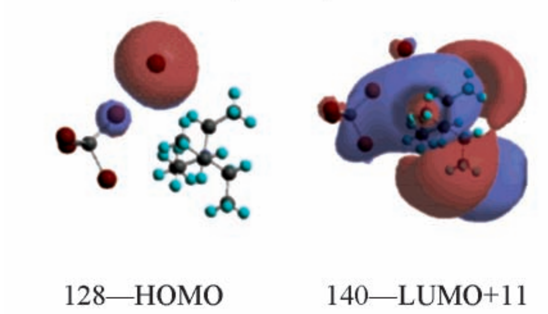

(c) orbitals of $[NEt_4I\cdot CBr_4]$

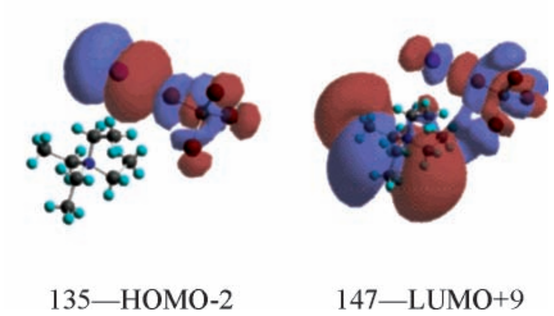

Figure 5. Orbitals contributing mostly to two-photon resonant states of $[NEt_4h\cdot CBr_4]$ ($h = Cl, Br, I$).

resonant state have some changes and the tetraalkylammonium group also takes part in the charge-transfer processes with a small amount s- and p-type atomic orbitals of N and C atoms on the alkyl group. Accordingly, enhancement of the TPA cross section $\delta(\omega)$ ascribes the strong charge transfer of the donor and acceptor and the larger π-electron delocalization in the considered molecules to the increased donor strengths.

4. Conclusions

In this paper, we employ the quantum chemical calculations of the time-dependent density functional theory (TDDFT) technique combined with the SOS method to investigate the two-photon absorption properties of a series of donor−acceptor chromophores such as tetraalkylammonium halide/carbon tetrabromide ($[NR_4h\cdot CBr_4]$, $h = Cl, Br, I$; $R = Me, Et, Pr$). The two-photon absorption spectra are theoretically modeled, and the electronic origins of these spectra are analyzed. The calculated results show that these charge-transfer complexes have large TPA cross sections and the $[NEt_4I\cdot CBr_4]$ has the largest TPA cross section δ among them with the value of 5.0×10^{-45} cm^4 s photon^{-1}. The maximum values of δ increase as the radii of the halide anions become larger in the order $Cl^- < Br^- < I^-$ for $[NEt_4h\cdot CBr_4]$ complexes, and for those through space interaction donor/acceptor dyads, δ values also increase with the increased separation distance between the donor/acceptor centers. However, when the donor is fixed as bromide, the TPA cross sections vary slightly as the size of the alkyl group increase from methyl to propyl. Whatever the atomic order number of the halogen or the size of the alkyl group increase, the largest δ value is localized at 520−690 nm and the maximum wavelength of the TPA peak, λ_{max}, indicates a bathochromic shift. To better understand the enhancement of the TPA in those molecules, we analyze the excited-state properties and the orbital characters and found that the electronic transition between the halide anion and the carbon tetrabromide makes a significant contribution to the excited states. It can be concluded for the investigated complexes that the electronic donor−acceptor charge transfer plays an important role for TPA activity, the TPA cross section $\delta(\omega)$ can be significantly enhanced by donor substituents and larger π-electron delocalization, whereas changes in the size of the alkyl group do not make a substantial contribution.

Acknowledgment. This investigation was based on work supported by the National Basic Research Program of China No2004CB720605, the National Natural Science Foundation of China under projects 20373073 and 90201015, the Science Foundation of the Fujian Province (No. E0210028), and the Foundation of State Key Laboratory of Structural Chemistry (No. 060007).

References and Notes

(1) Ahn, T. K.; Kim, K. S.; Kim, D. Y.; Noh, S. B.; Aratani, N.; Ikeda, C.; Osuka, A.; Kim, D. *J. Am. Chem. Soc.* **2006**, *128*, 1700.

(2) Nielsen, C. B.; Rettrup. S.; Sauer, S. P. *J. Chem. Phys.* **2006**, *124*, 114108.

(3) Ohta, K.; Kamada, K. *J. Chem. Phys*. **2006**, *124*, 124303.

(4) Rubio-Pons, Ò.; Luo, Y.; Agren, H. *J. Chem. Phys.* **2006**, *124*, 094310.

(5) Oliveira, S. L.; Corrêa, D. S.; Boni, L. De.; Misoguti, L.; Zilio, S. C.; Mendonça, C. R. *Appl. Phys. Lett.* **2006**, *88*, 021911.

(6) Herda, R.; Hakulinen, T.; Suomalainen, S.; Okhotnikov, Oleg. G. *Appl. Phys. Lett.* **2005**, *87*, 211105.

(7) He, G. S.; Bhawalkar, J. D.; Zhao, C.-F.; Prasad, P. N. *Appl. Phys. Lett.* **1995**, *67*, 2433.

(8) Ehrlich, J. E.; Wu, X. L.; Lee, I.-Y. S.; Hu, Z.-Y.; Röckel, H.; Marder, S. R.; Perry, J. W. *Opt. Lett.* **1997**, *22*, 1843.

(9) Larson, D. R.; Zipfel, W. R.; Williams, R. M.; Clark, S. W.; Bruchez, M. P.; Wise, F. W.; Webb, W. W. *Science* **2003**, *300*, 1434.

(10) Denk, W.; Strickler, J. H.; Webb, W. W. *Science* **1990**, *248*, 73.

(11) Xu, C.; Zipfel, W.; Shear, J. B.; Williams, R. M.; Webb, W. W. *Proc. Natl. Acad. Sci. U.S.A.* **1996**, *93*, 10763.

(12) Bhawalkar, J. D.; Kumar, N. D.; Zhao, C. F.; Prasad, P. N. *J. Clin. Laser Med. Surg.* **1997**, *15*, 201.

(13) Strickler, J. H.; Webb, W. W. *Opt. Lett.* **1991**, *16*, 1780.

(14) Cumpston, B. H.; Ananthavel, S. P.; Barlow, S.; Dyer, D. L.; Ehrlich, J. E.; Erskine, L. L.; Heikal, A. A.; Kuebler, S. M.; Lee, I.-Y. S.; McCord-Maughon, D.; Qin, J.; Röckel, H.; Rumi, M.; Wu, X.-L.; Marder, S. R.; Perry, J. W. *Nature* **1999**, *398*, 51.

(15) Zhou, W. H.; Kuebler, S. M.; Braun, K. L.; Yu, T. Y.; Cammack, J. K.; Ober, C. K.; Perry, J. W.; Marder, S. R. *Science* **2002**, *296*, 1106.

(16) Parthenopoulos, D. A.; Rentzepis, P. M. *Science* **1989**, *245*, 843.

(17) Belfield, K. D.; Schafer, K. J. *Chem. Mater.* **2002**, *14*, 3656

(18) Reinhardt, B. A.; Brott, L. L.; Clarson, S. J.; Dillard, A. G.; Bhatt, J. C.; Kannan, R.; Yuan, L. X.; He, G. S.; Prasad, P. N. *Chem. Mater*. **1998**, *10*, 1863.

(19) Heikal, A. A.; Huang, S. H.; Halik, M.; Marder, S. R.; Wenseleers, W.; Perry, J. W.; Webb, W. W. *Biophys. J.* **2002**, *82*, 493A.

(20) Pond, S. J. K.; Rumi, M.; Levin, M. D.; Parker, T. C.; Beljonne, D.; Day, M. W.; Brédas, J. L.; Marder, S. R.; Perry, J. W. *J. Phys. Chem. A* **2002**, *106*, 11470.

(21) Werts, M. H. V.; Gmouh, S.; Mongin, O.; Pons, T.; Blanchard-Desce, M. *J. Am. Chem. Soc.* **2004**, *126*, 16294.

(22) Rumi, M.; Ehrlich, J. E.; Heikal, A. A.; Perry, J. W.; Barlow, S.; Hu, Z. Y.; McCord-Maughon, D.; Parker, T. C.; Röckel, H.; Thayumanavan, S.; Marder, S. R.; Beljonne, D.; Brédas, J. L. *J. Am. Chem. Soc.* **2000**, *122*, 9500.

(23) Albota, M.; Beljonne, D.; Brédas, J.-L.; Ehrlich, J. E.; Fu, J.-Y.; Heikal, A. A.; Hess, S. E.; Kogej, T.; Levin, M. D.; Marder, S. R.; McCord-Maughon, D.; Perry, J. W.; Röckel, H.; Rumi, M.; Subramaniam, G.; Webb, W. W.; Wu, X.-L.; Xu, C. *Science* **1998**, *281*, 1653.

(24) Kauser, W.; Garrett, C. G. B. *Phys. Rev. Lett.* **1961**, *7*, 229.

(25) Rogers, J. E.; Slagle, J. E.; McLean, D. G.; Sutherland, R. L.; Sankaran, B.; Kannan, R.; Tan, L.-S.; Fleitz, P. A. *J. Phys. Chem. A* **2004**, *108*, 5514.

(26) Zojer, E.; Beljonne, D.; Kogej, T.; Vogel, H.; Marder, S. R.; Perry, J. W.; Brédas, J. L. *J. Chem. Phys.* **2002**, *116*, 3646.

(27) Pond, S. J. K.; Tsutsumi, O.; Rumi, M.; Kwon, O.; Zojer, E.; Brédas, J. L.; Marder, S. R.; Perry, J. W. *J. Am. Chem. Soc.* **2004**, *126*, 9291.

(28) Morel, Y.; Irimia, A.; Najechalski, P.; Kervella, Y.; Stephan, O.; Baldeck, P. L.; Andraud, C. *J. Chem. Phys.* **2001**, *114*, 5391.

(29) Katan, K. C.; Terenziani, F.; Mongin, O.; Werts, M. H. V.; Porres, L.; Pons, T.; Mertz, J.; Tretiak, S.; Blanchard-Desce, M. *J. Phys. Chem. A* **2005**, *109*, 3024.

(30) Chung, S.-J.; Kim, K.-S.; Lin, T.-C.; He, G. S.; Swiatkiewicz, J.; Prasad, P. N. *J. Phys. Chem. B* **1999**, *103*, 10741.

(31) Adronov, A.; Fréchet, J. M.; He, G. S.; Kim, K.-S.; Chung, S.-J.; Swiatkiewicz, J.; Prasad, P. N. *Chem. Mater.* **2000**, *12*, 2838.

(32) Hurst, S. K.; Humphrey, M. G.; Isoshima, T.; Wostyn, K.; Asselberghs, I.; Clays, K.; Persoons, A.; Samoc, M.; Luther-Davies, B. *Organometallics* **2002**, *21*, 2024.

(33) Strieter, F. J.; Templeton, D. H. *J. Chem. Phys.* **1962**, *37*, 161.

(34) Lindeman, S. V.; Hecht, J.; Kochi, J. K. *J. Am. Chem. Soc.* **2003**, *125*, 11597.

(35) Blackstock, S. C.; Lorand, J. P.; Kochi, J. K. *J. Org. Chem.* **1987**, *52*, 1451.

(36) Blackstock, S. C.; Kochi, J. K. *J. Am. Chem. Soc.* **1987**, *109*, 2484.

(37) Stratmann, R. E.; Scuseria, G. E.; Frisch, M. J. *J. Chem. Phys*. **1998**, *109*, 8218.

(38) Bauemschmitt, R.; Ahlrichs, R.*Chem. Phys. Lett.* **1996**, *256*, 454.

(39) Casida, M. E.; Jamorski, C.; Casida, K. C.; Salahub, D. R. *J. Chem. Phys.* **1998**, *108*, 4439.

(40) Orr, B. J.; Ward, J. F. *Mol. Phys.* **1971**, *20*, 513.

(41) Pierce, B. M. *J. Chem. Phys.* **1989**, *91*, 791.

(42) van Gisbergen, S. J. A.; Snijders, J. G.; Baerends, E. J.; *Comput. Phys. Commun.* **1999**, *118*, 119.

(43) Wu, D.-S.; Cheng, W.-D.; Li, X.-D.; Lan, Y.-Z.; Chen, D.-G.; Zhang, Y.-C.; Zhang, H.; Gong, Y.-J. *J. Phys. Chem. A* **2004**, *108*, 1837.

(44) Cheng, W.-D.; Wu, D.-S.; Zhang, H.; Li, X.-D.; Lan, Y.-Z.; Chen, D.-G.; Wang, H.-X. *J. Chem. Phys.* **2003**, *119*, 13100.

(45) Dick, B.; Hochstrasser, R. M.; Trommsdorff, H. P. *Nonlinear Optical Properties of Organic Molecules and Crystals*; Chemla, D. S., Zyss, J., Eds.; Academic Press: Orlando, FL, 1987; Vol. 2, pp 167−170.

(46) Li, X.-D.; Cheng, W.-D.; Wu, D.-S.; Lan, Y.-Z.; Zhang, H.; Gong, Y.-J.; Li, F.-F.; Shen, J. *J. Chem. Phys.* **2004**, *121*, 5885.

(47) Atkins, P. W. *Molecular Quantum Mechanics*, 2nd ed.; Oxford University Press: New York, 1983; Chapter 11.